

We are IntechOpen, the world's leading publisher of Open Access books Built by scientists, for scientists

6,900

Open access books available

186,000

International authors and editors

200M

Downloads

Our authors are among the

154

Countries delivered to

TOP 1%

most cited scientists

12.2%

Contributors from top 500 universities



WEB OF SCIENCE™

Selection of our books indexed in the Book Citation Index
in Web of Science™ Core Collection (BKCI)

Interested in publishing with us?
Contact book.department@intechopen.com

Numbers displayed above are based on latest data collected.
For more information visit www.intechopen.com



Improving the Light-Emitting Efficiency of GaN LEDs Using Nanoimprint Lithography

Yeeu-Chang Lee¹ and Sheng-Han Tu²

¹*Department of Mechanical Engineering, Chung Yuan Christian University*

²*Genesis Photonics Inc.*

Taiwan

1. Introduction

A light-emitting diode (LED) is an electroluminescent device with a broad selection of emission wavelengths (colors). The unique properties of LEDs, such as compactness, low power consumption, long lifetime, and fast turn-on time have made LEDs an indispensable component in modern traffic lighting, display, car lighting, and cell phones applications. In recent years, LED usage has grown more rapidly due to the application of backlights in large-size flat panel displays, a market previously dominated by CCFL. In addition, wide speculation foresees that the next boom for LEDs could arise from the interior/exterior lighting market. As shown in U.S. energy consumption statistics conducted by the U.S. government, the energy consumption for interior/exterior lighting occupies 22%~25% of the total electrical energy produced in the U.S. Using LEDs to replace all traditional interior/exterior lighting used today can save at least an estimated amount of 20 billion U.S. dollars in annual energy costs while also significantly reducing carbon emission. Therefore, LEDs have attracted a large amount of investments from corporations in Asia, North America, and Europe, aiming to develop reliable processes to improve the production yield and optical efficiency of LEDs.

The nanoimprint lithography is a nanoscale structural formation technique with highly reproducible patterns, and is therefore suitable for LED fabrication. The typical length scale of structures for applications of LEDs ranges from a few hundred nanometers to a few micrometers, which is roughly on par with the resolution limit of the traditional optical lithography technology. Though a higher resolution is attainable using the stepper projection lithography method, the corresponding higher process cost renders the fabricated LEDs less economical. Unlike the integrated circuit, the micro- and nanostructures of an LED are often simple 2D periodic patterns. Once an imprinting mold with a high accuracy and precision is made from techniques such as the stepper projection lithography (or alternatively the electron beam, the ion beam, and the interference lithography), the LED patterns can be massively reproduced. This article discusses the role of the precision nanoimprint lithography for improving the optical efficiency of LEDs.

2. Limits and enhancements of the light-extraction efficiency of GaN LEDs

No single semiconductor material alone is capable of emitting white light. A white light LED typically consists of an appropriate mixture of (a) red, blue, and green LEDs, or (b) blue

and yellow lights, where the blue LED stimulating yellow phosphor produces the yellow light. In either case, the blue LED is the main constituent of a white light LED. Most blue LEDs are made from GaN, the compound discussed in this paper.

2.1 Analysis of the light extraction efficiency

Excluding the substrate, a typical LED structure is only a few micrometers thick. The region capable of emitting light is called the active region, composed of multiple quantum wells (MQWs) of less than 1 μm in thickness. The active region can be regarded as a thin film containing a large number of point light sources radiating photons in all directions. The ratio of the number of these emitted photons to the number of electrons injected to excite the quantum wells constitutes an essential figure (also known as internal quantum efficiency) for judging the performance of an LED. Another significant figure of value concerns the number of photons out of the active region that can be extracted to the free space. This is called the light extraction efficiency, $\eta_{\text{extraction}}$, defined as follows:

$$\eta_{\text{extraction}} = \frac{\text{\# of photons emitted into free space per second}}{\text{\# of photons emitted from active region per second}}$$

The extraction efficiency is definitely not 100%. In practice, reflection at the interface between two materials with different refractive indices is unavoidable. This reflection can be considered as a loss (also known as Fresnel loss) mechanism in the LED. However, the main loss channel in the LED is caused by the total internal reflection (TIR). TIR is an optical phenomenon that occurs when the light enters from an optically dense medium to a less optically dense medium, such as when the light exits from GaN and enters the air. As the angle of incidence is greater than the critical angle, no light can be transmitted at the interface and all light is reflected. Snell's law is used to determine the critical angle:

$$n_s \sin \theta_1 = n_{\text{air}} \sin \theta_2$$

where n_s and n_{air} are the refractive indices of GaN and air, respectively. θ_1 is the angle of incidence and θ_2 is the refraction angle. When the refraction angle is greater than 90° , which forbids photons from being transmitted at the interface, the corresponding angle of incidence is the critical angle, $\theta_c = \sin^{-1}\left(\frac{n_{\text{air}}}{n_s}\right)$, as shown in Figure 1- Left.

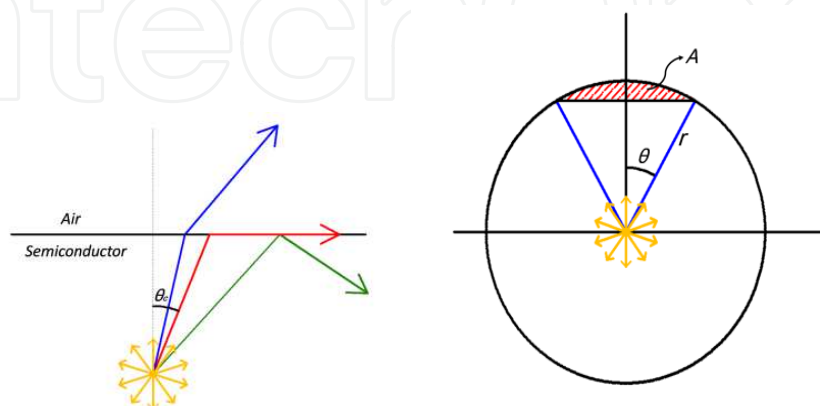


Fig. 1. (Left) The critical angle for the total internal reflection (Right) The light emission cone of an LED

For instance, the refraction index of GaN at room temperature is 2.4, corresponding to a critical angle of 24.6°. When the angle of incidence (regarding air) of the point light sources in the active region of the GaN LED is smaller than 24.6°, all emitted photons can be delivered to the free space.

In 3D space, the point light sources emit photons isotropically in spherical directions. The radiation area is the area of the sphere $4\pi r^2$, where r is the distance from the wavefront to the point light source. When the spherical wavefront reaches the GaN/air interface, only the photons within the conical region (using the critical angle as the solid angle) can escape the semiconductor (Figure1- Right). The radiation area of the escaping cone is:

$$A = \int dA = \int_{\theta=0}^{\theta_c} 2\pi r \sin \theta r d\theta = 2\pi r^2 (1 - \cos \theta_c)$$

The emitted optical power per unit area of the escaping cone is equal to the power per unit area of the emission sphere of the point source:

$$\frac{P_{escape}}{2\pi r^2 (1 - \cos \theta_c)} = \frac{P_{source}}{4\pi r^2}$$

$$P_{escape} = P_{source} \frac{2\pi r^2 (1 - \cos \theta_c)}{4\pi r^2} = P_{source} \frac{(1 - \cos \theta_c)}{2}$$

$$\frac{P_{escape}}{P_{source}} = \frac{(1 - \cos \theta_c)}{2}$$

By expanding the cosine term into power series, the following equation can be derived:

$$\frac{P_{escape}}{P_{source}} \approx \frac{1}{2} \left[1 - \left(1 - \frac{\theta_c^2}{2!} + \frac{\theta_c^4}{4!} - \dots \right) \right]$$

For semiconductors with high refraction indices, the critical angle is small. Therefore, the high order terms in the above equation can be neglected, leading to the following:

$$\frac{P_{escape}}{P_{source}} \approx \frac{1}{4} \theta_c^2$$

Using GaN as an example once more, the light extraction efficiency (calculated below) from the surface of the active region to the air is only 4.61%.

$$\frac{P_{escape}}{P_{source}} \approx \frac{1}{4} \theta_c^2 = \frac{1}{4} \times \left(\frac{24.6}{180} \times \pi \right)^2 \approx 4.61\%$$

2.2 Methods to improve the light extraction efficiency

Numerous methods have been proposed to circumvent the poor light extraction efficiency imposed by the TIR effect. Modifying the geometry of the LED chip is one such method [1-3]. By shaping the sides of the LED chip into trapezoidal (or up-side-down trapezoidal)

shapes, the TIR effect from the top and the sides of the chip can be released. However, the typical thickness of a blue LED chip (including the substrate) is only approximately 90 μm , rendering the shaping of the sides an extremely difficult task. Another common method to reduce the TIR effect is by roughening the sides and the surface of the LED chip [4,5], which can enhance the scattering effect. As shown in Figure 2, the light is extracted whenever the guided light reaches the roughened interface. However, the roughening technique also degrades the electrical characteristics of the LED, causing the forward voltage to rise. If the electrical issue can be resolved, the roughening technique could be a simple and reliable solution.

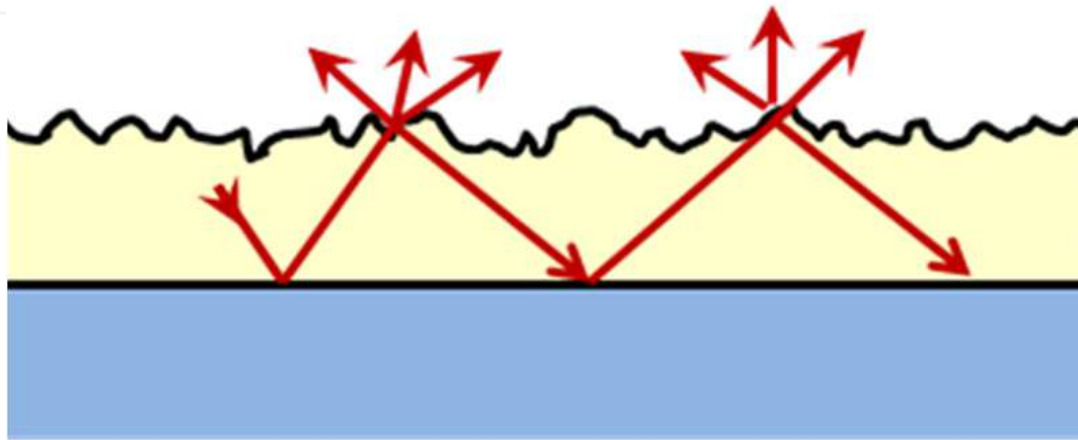


Fig. 2. Reducing the TIR by scattering

Lee et al. [6, 7] simulated the effects of the surface structures, including the size and shape effects of these structures under different packaging conditions, on the light extraction efficiency of the LED, using ray tracing. However, the ray tracing technique only applies when the size of the structures is much bigger than the wavelength of the light. For structures that are close to the size of the photon wavelength, diffraction occurs. Though the wave nature of the light can be simulated by the FDTD or the RCWA methods, the applicability of these methods to the particle-wave duality nature of the light (prominent for sub-wavelength structures) requires further evaluation.

The most commonly used substrate for growing GaN films is sapphire. However, a 16% lattice mismatch between the GaN and the sapphire exists, causing a large number of threading dislocations ($10^9 \sim 10^{12} \text{ cm}^{-2}$) at the interface. Theoretically, these threading dislocations could extend from the epitaxial interface to the top of the p-GaN surface, leading to undesirable outcomes for the quality and lifetime of the LED chip. An approach to solving this problem requires altering the crystal growth orientation of the epitaxial film grown on etching surface structures of sapphire substrates. The interrupted and/or bent dislocations can reduce the density of the threading dislocations. In addition, these surface structures can display effects similar to the roughened surface to enhance the light extraction efficiency for the multiple reflections at the GaN/sapphire interface as shown in Figure 3, to cause guided light escape to free space while suppressing the TIR. Such substrate patterning is known as the patterned sapphire substrate (PSS) technique [8-11]. PSS is a popular technique for enhancing LED efficiency. Typical PSS patterns are on the order of micrometers, and shrinking the size of the patterns into nanoscales (also known as NPSS) is believed to significantly improve efficiency.

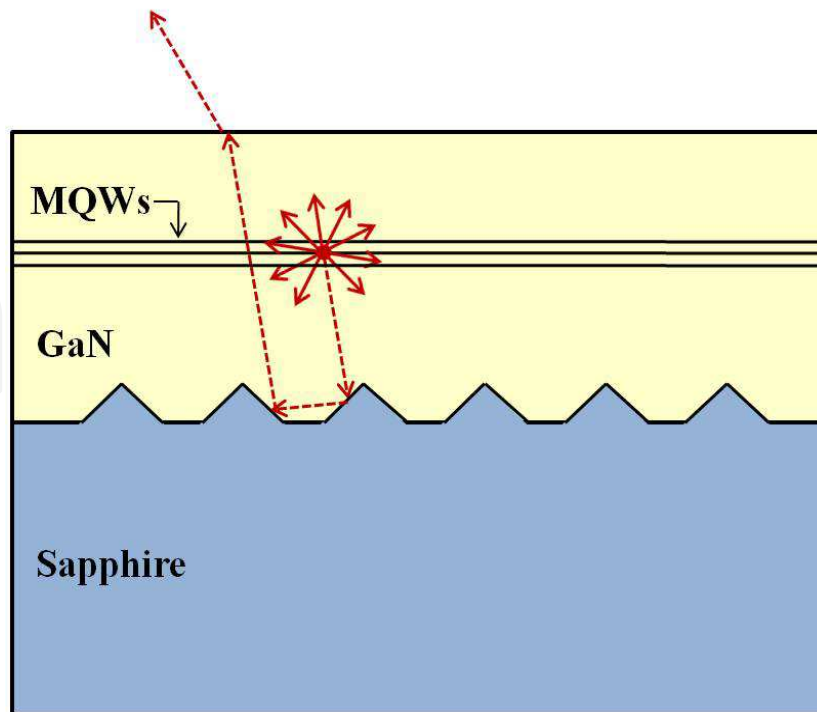


Fig. 3. Possible path for the light traveling in the patterned sapphire substrates (PSS) LED

In 1987, Eli Yablonovitch [12] and Sajeev John [13] discovered that electromagnetic waves transmission is disallowed in certain periodically patterned structures (now called photonic crystals). This phenomenon is similar to electrons in the forbidden band of an energy band diagram in solids. Much research has since focused on utilizing the photonic crystal effect. Early applications of the photonic crystal effect were in the optical communication, where the photonic bandgap was used to create a waveguide of extremely large bending angles. More recently, the photonic crystal effect has also been applied to the LED. The photonic crystal can be used to enhance the external quantum efficiency of the LED by (a) forming a photonic bandgap within the LED chip, thereby forcing the generated photons to exit the chip and/or (b) forming an efficient waveguide to couple photons to the free space. Except to enhance the light extraction efficiency, photonic crystals can also modify far-field light pattern of the LED. The far-field light pattern is related to the information transmission of traffic lights [14], fiber coupling efficiency of LED sources [15], and the color mixing homogeneity in LED displays[16], etc. Therefore, the combination of the photonic crystal and the LED has widespread application.

3. Discussions of the nanoimprint techniques

Based on the aforementioned analysis, the light-emitting efficiency of the LED can be improved by fabricating micro- or nanostructures inside or on the surface of the chip/substrate. The small dimension patterns can be fabricated via nanoimprint lithography. The advantages of nanoimprint lithography are fast production and the low cost, which satisfy industry production requirements. In addition, the method simplifies the complex optical lithography, freeing it from the diffraction limit. The nanoimprint lithography was regarded as one of the ten emerging technologies in 2003 with the potential to change the world.

Nanoimprint lithography can be distinguished in three types: hot embossing nanoimprint lithography (HE-NIL), UV-curing nanoimprint lithography (UV-NIL), and soft imprint lithography (SIL). A schematic diagram of the three imprint types is shown in Figure 4:

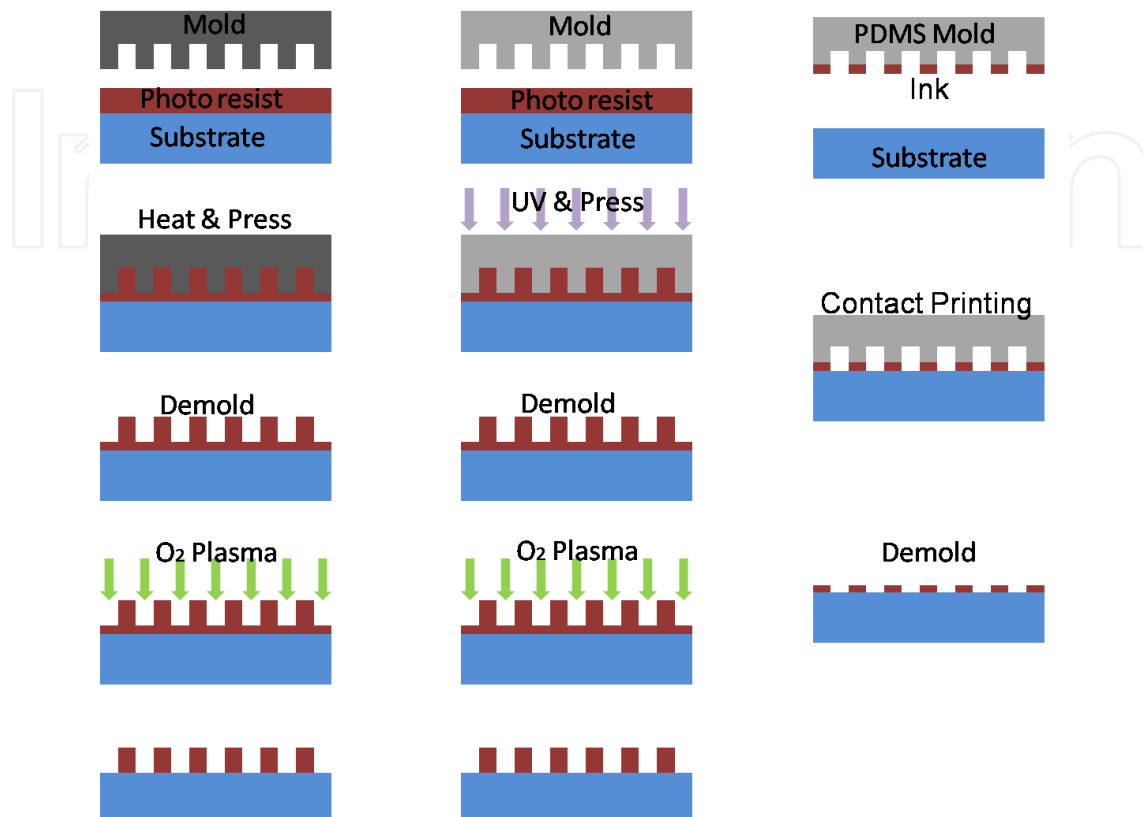


Fig. 4. Schematics of the hotembossing nanoimprint lithography, the UV-curing nanoimprint lithography, and the soft nanoimprint lithography (from left to right, respectively)

Steven Y. Chou from Princeton University developed the first hot embossing nanoimprint lithography in 1995 [17]. The electron beam lithography and etching were used to fabricate a template pattern on a silicon mold. Under a temperature of 200 °C and a pressure of 1900 psi, the silicon mold was pressed into a thermoplastic polymer called poly(methyl methacrylate) (PMMA). When the temperature was above its glass transform temperature (T_g), the PMMA became rubber-like and started to fill the pattern on the silicon mold. When the temperature dropped below T_g , the PMMA transformed into a high mechanical strength and glass-like material. Once the mold was separated from the sample, dry etching was used for cleaning the PMMA residues to complete the process. A disadvantage of the hot embossing nanoimprint lithography is that the nanostructures are fabricated under high temperature and high-pressure environments, and hence, its structure is prone to changes in temperature. Another disadvantage is the limitation of the application due to the requirement of long thermal cycle during the process.

The UV-curing nanoimprint lithography [18] uses UV-light to solidify the imprint material. A highly UV transparent and hard quartz is selected as the mold material. Quartz mold is pressed into the imprinting material to transfer the pattern into the silicon substrate at room temperature. The imprinting material is then irradiated with UV light, resulting in a cross-

link of the material. After detachment of the mold, dry etching is used for cleaning the residual layer to complete the process. The UV-curing nanoimprint lithography is realized under room temperature and at a low pressure, and therefore, has the advantage of fast production and of being a simple process. However, its disadvantage is that the mold or substrate material must be UV-transparent (e.g., quartz, aluminum oxide).

In the research of soft nanoimprint lithography [19], a soft polymer such as polydimethylsiloxane (PDMS) is used as the mold to duplicate the pattern of hard mold. Acting like a stamp wetted with ink, PDMS mold is wetted with an ink made of, for instance, the self-assembly monomer (SAM). Alternatively, the substrate could also be sprayed with the imprint material. By compressing the PDMS soft mold and the substrate, the pattern of the mold is imprinted to the substrate. The soft nanoimprint lithography, similar to the UV-curing nanoimprint lithography, has the advantages of fast production, simple process, and low equipment cost. The key benefit of the soft nanoimprint lithography is its flexible mold, which makes it suitable for the non-planar imprint process, thereby having wider application. The disadvantage is that the mechanical strength of the mold is relatively weak compared to that of the others, resulting in easy wearing of the imprint patterns or the molds. To improve the imprint technique, a reversal imprint is developed. As shown in Figure 5, the aforementioned imprint techniques place the imprinting materials on the substrate surface. Conversely, the reversal imprint technique places the imprinting material on the surface of the mold before the entire material is pressed for transferring to the substrate. This procedure is similar to “planting” structures on the substrate, and the force required for the reversal imprint is comparably smaller. A 3D structure can be fabricated by stacking the structures layer-by-layer using the reversal imprint technique [20]. A successful reversal imprint requires the imprinting material to be hydrophilic to the substrate and hydrophobic to the mold, thereby enabling completion of the demolding process. Figure 5 shows the PTFE placed on the mold and the substrate preprocessed via HMDS. The attractive/repulsive surface of the materials can be analyzed by measuring the contact angle.

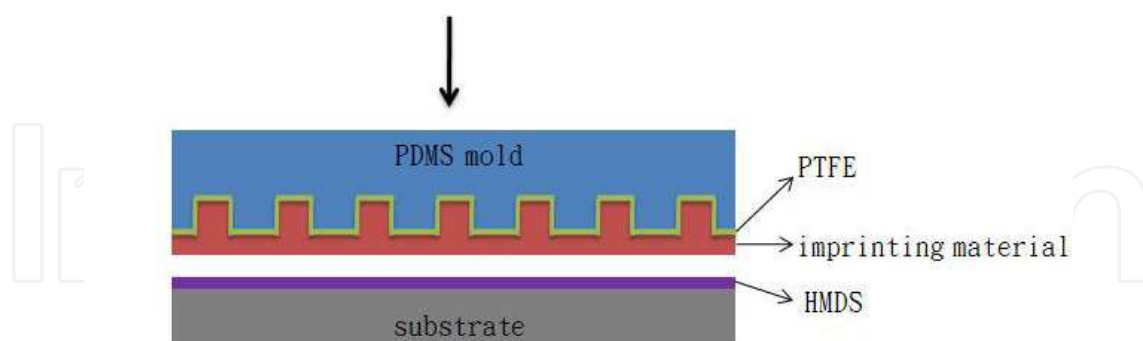


Fig. 5. Schematic diagram of the reversal imprint

Various nanoimprinting techniques have been developed to improve the abovementioned imprint processes. Among them, the roller imprint technique, originating from the roller press of the plastic sheets, is applied for nanoimprint. For example, a roller with nanostructures on its surface is rotated on a substrate composed of the thermoplastic polymer. When the temperature is set above the glass transition temperature, the thermoplastic polymer is in conjunction with the structures on the roller [21]. The nanostructure on the roller can be fabricated by the electroplating nickel mold technique,

which applies nickel film on the roller [22, 23]. If the substrate is flexible, structures can be reproduced massively via continuous roll-to-roll process. This method is suitable for the thermoplastic polymer films. The diffuser film used for current backlights of TFT-LCD panel can be fabricated via roll-to-roll process transferring of the microstructure to the PET film by roller imprint. The roller imprint, in practice, can adapt a process similar to the aforementioned imprint process. That is, PDMS soft mold is applied over the surface of the quartz roller, thereby enabling the continuous imprinting process, as shown in Figure 6. [24]. Various light sources can be used to harden the imprint material. For example, the hot embossing imprint can be heated up rapidly using an infrared light or an infrared laser [25]. The UV-hardening can be achieved via the UV light or UV laser. Using the laser has the benefit of using optical lenses to focus the beam to the ideal imprint area. Continuous imprinting process is demonstrated using the roller imprint method. Instead of imprinting the entire surface at once, the roller and the substrate are imprinted progressively, rendering the roller imprint useful for the fabrication of structures on a large surface.

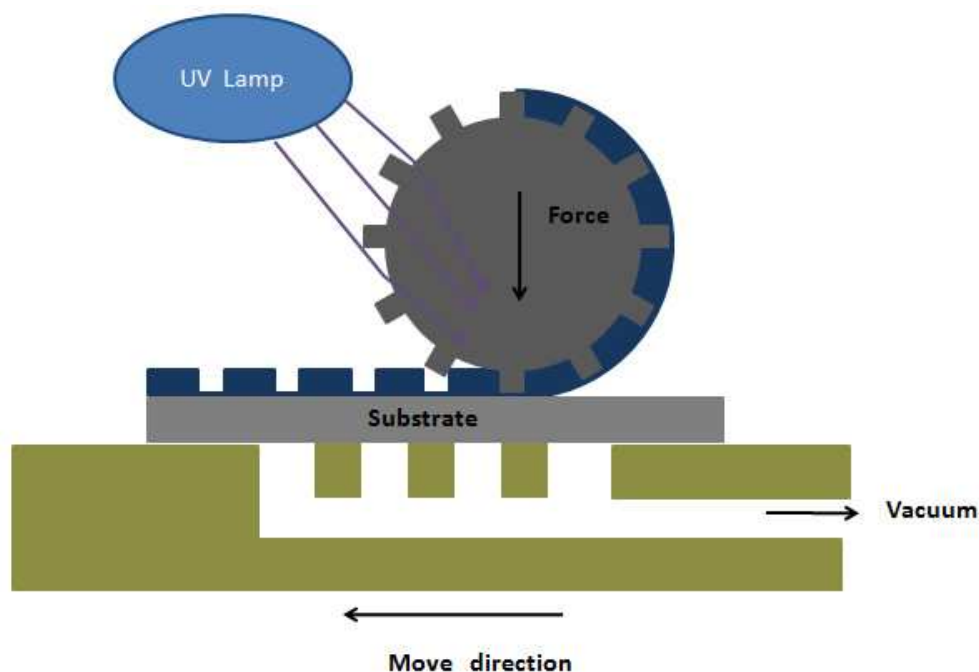


Fig. 6. Schematics of the UV-assisted roller imprint equipment

4. Improvement of the light-emitting efficiency by the imprint structure

4.1 The Effect of surface structures

As previously discussed, the light-emitting efficiency can be improved by a roughened surface, which can be achieved by the imprint of a surface structure. A uniform size and the periodicity of the structures benefit the homogeneity of the emitted light. In 2007, Chang et al. [26] applied hot embossing nanoimprint lithography to imprint the PMMA into a transparent conductive layer ITO of an LED. Inductively coupled plasma (ICP) etching was used for cleaning the process residues to expose the ITO, followed by etching in hydrochloric acid to produce periodic ITO holes, which were 90nm in depth, 0.85 μm in diameter, and 0.5 μm in spacing. Compared to conventional LEDs, the periodic structure of

an LED with size $350 \times 350 \mu\text{m}^2$ showed a 12% improvement in the light-emitting efficiency with an input current of 20 mA. Huang et al. [27] fabricated p-GaN nanostructures on the surface of a $1 \times 1 \text{ mm}^2$ high-power green LED chip. A SiO_2 thin film was first deposited onto p-GaN, and a silicon mold was used for the hot embossing imprint process. Reactive ion etching (RIE) was used for cleaning the residues of the imprinting material and SiO_2 , to complete the transferring of the structure using SiO_2 as the resist. A p-GaN nanostructure of 75 nm depth was later produced via ICP etching. The residual SiO_2 was removed using a buffer oxidation etchant (BOE). Finally, an ITO thin film was deposited onto p-GaN. Due to high scattering effect, the light-emitting efficiency of the nanostructured LED was 48% higher than that of conventional LEDs with an input current of 350 mA. Zhou et al. [28] used the soft UV-nanoimprint lithography to fabricate nanostructures onto a $1 \times 1 \text{ mm}^2$ p-GaN high-efficiency LED chip. A porous membrane mold with a nanohole approximately 100 nm in size was first fabricated using the anodic aluminum oxide (AAO) method. A two-inch PDMS soft mold was replicated for UV-nanoimprint process. The process followed was similar to that of Huang et al. [27]. The light-emitting efficiency of the unpackaged nanostructured LED chip was 10.9% higher than that of conventional LEDs with an input current of 350 mA. The enhancement of efficiency would be 48% when the LED chip is packaged.

Other than the imprint method that imprints structures onto the LED surface via etching, Lee et al. [29] fabricated the microstructure directly onto the ITO. Figure 7 is the SEM image of the one-dimensional and two-dimensional imprint structures. The imprinting material is not a conventional polymer, but is a spin on glass (SOG), which is similar to SiO_2 . The chemical and mechanical properties of this material are superior when compared to the polymer.

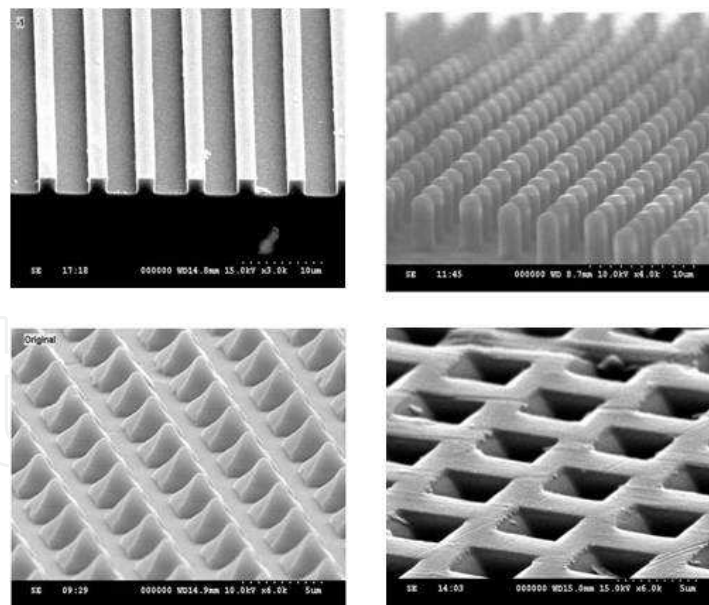


Fig. 7. SEM images of the one-dimensional and the two-dimensional imprint structures

Figure 8 is the schematic diagram that combines the imprint and the conventional LED fabrication process. The mesa etching (to expose the n-GaN) was first achieved using ICP. The electrode patterns were defined and deposited with p-type and n-type electrodes to fabricate conventional LED chips. After the hot embossing imprint process, the imprinting material on the electrodes was removed. Finally, the electrical and optical properties of the

LED were then measured. The results showed the forward bias of the imprinted LED is extremely similar to that of the conventional LED. Compared to the electrical property of the LED fabricated by etching above the p-GaN, the electrical property of the LED produced via this method was not damaged.

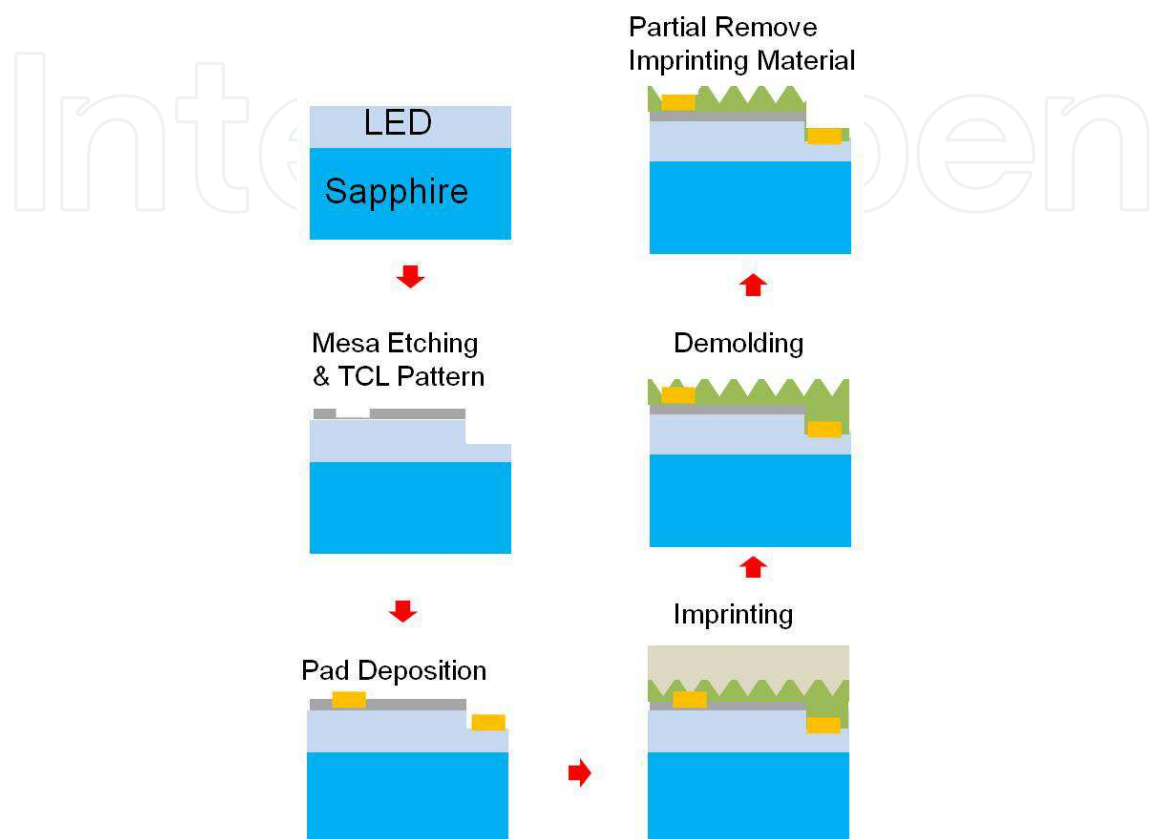


Fig. 8. Process flow of the conventional LED chip and imprint process

Regarding optical property, for a size of $300 \times 300 \mu\text{m}^2$, composed of a cylinder array $3 \mu\text{m}$ in diameter and $2 \mu\text{m}$ in spacing of the LED chip, the efficiency enhancement is 26.2% with 20 mA current. Figure 9 is the diagram that illustrates the possible optical paths of a light incident to cylinder and pyramid structures, showing that the surface structures are beneficial to ruin total internal reflection.

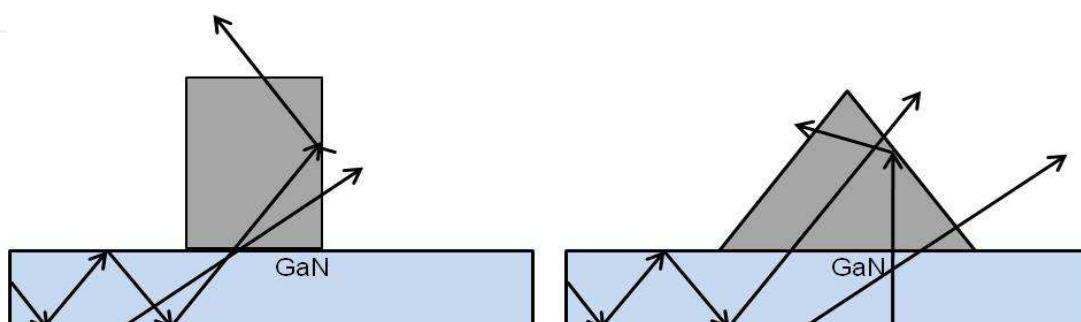


Fig. 9. The possible optical routes of an LED light incident to a micro-cylinder and to a pyramid structure

Comparing the micro-pyramid-structured LED ($3\ \mu\text{m}$ width and $2\ \mu\text{m}$ spacing) with the nano-pyramid-structured LED ($750\ \text{nm}$ width and $500\ \text{nm}$ spacing), the light output power of the nano-pyramid-structured LED, which has a more densified structure, is superior to that of the micro-pyramid-structured LED as the input current increases (Figure 10.) [30].

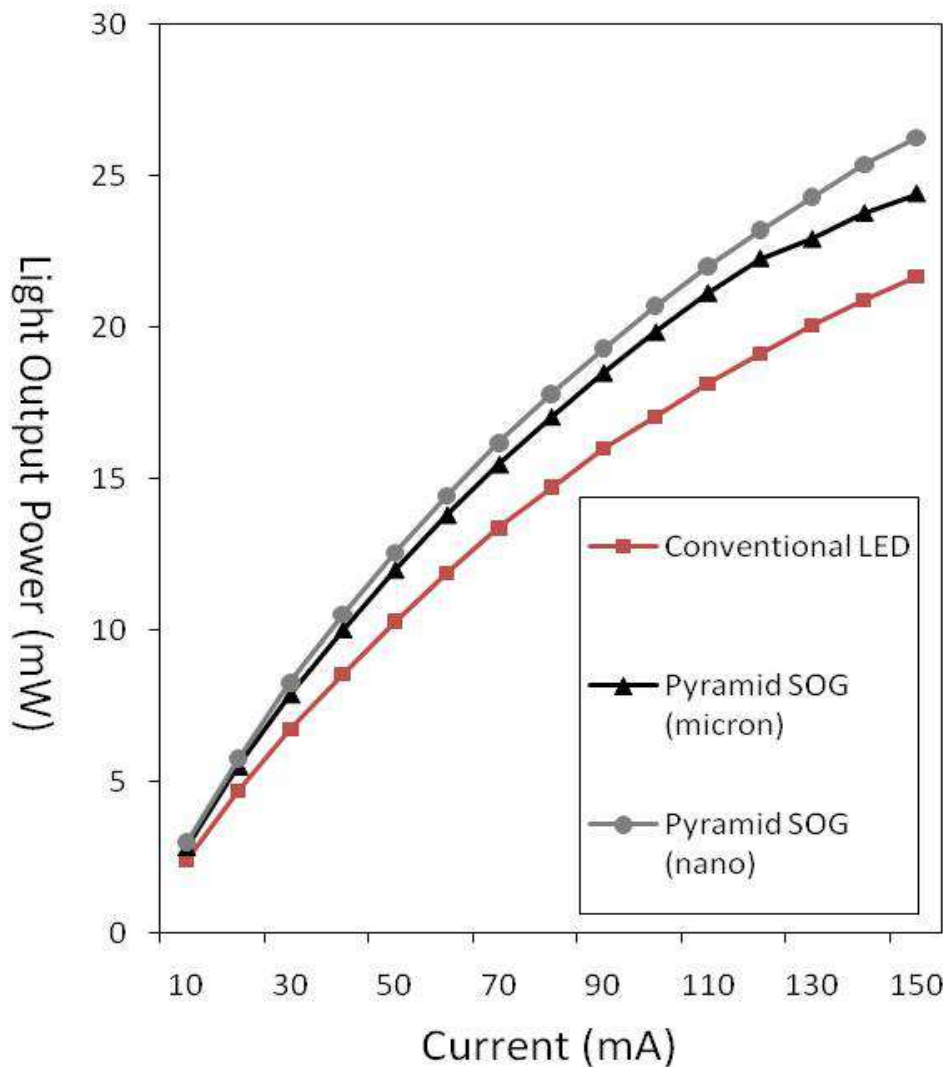


Fig. 10. A comparison of the light output powers of the microstructured, nanostructured, and conventional LEDs.

The study of the roller imprint in the application of fabricating LEDs is shown in Figure 11. The light output power of the micro-cylinders with different heights increases in conjunction with the current. Theoretically, taller cylinder LED has more surface area to emit light compared to the short cylinder. However, as shown in the results, the light output power was higher for the imprint cylinder-structured LED with $3\ \mu\text{m}$ diameter, $2\ \mu\text{m}$ spacing, and $1.5\ \mu\text{m}$ height, compared to the cylinder-structured LED with $2.5\ \mu\text{m}$ or $5.0\ \mu\text{m}$ height. This is because of the light absorption from the imprinting material, and thus, an optimal height of the imprint structure exists that maximizes the light emitting efficiency [24].

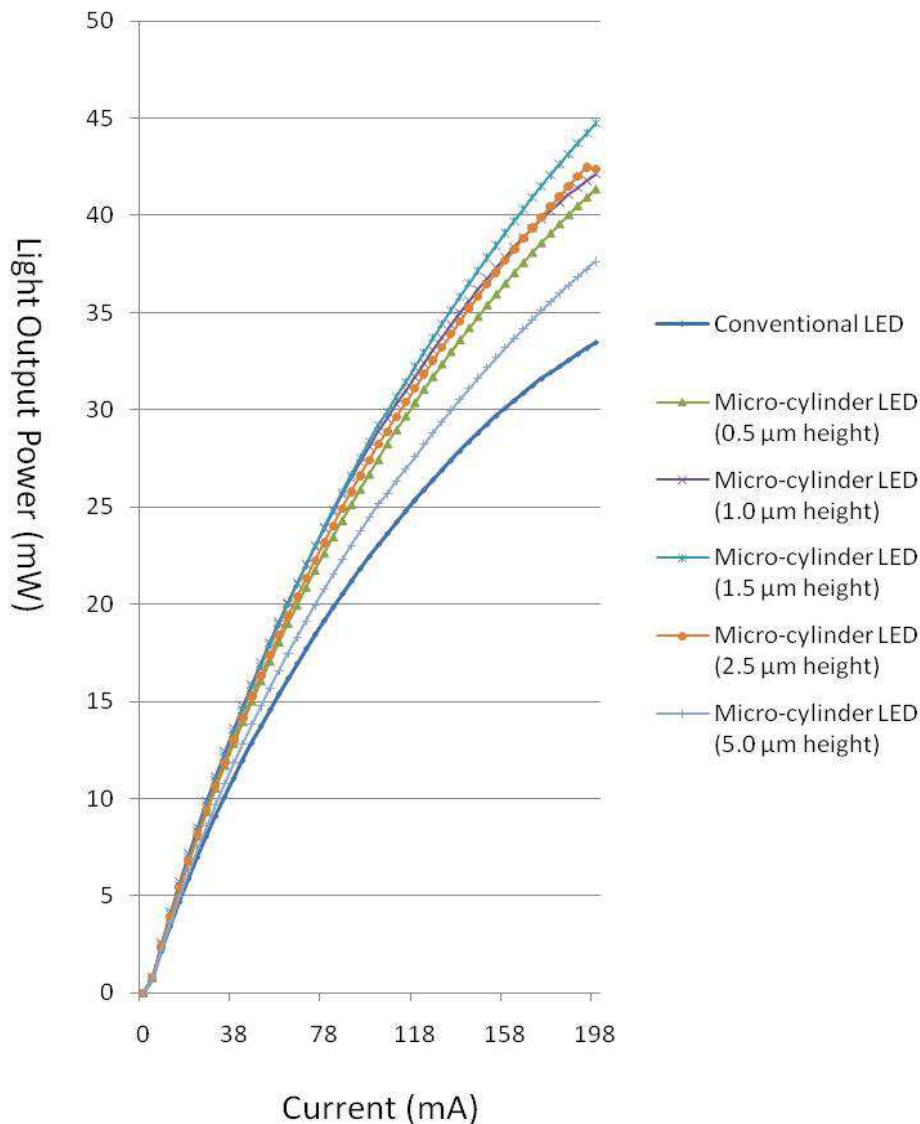


Fig. 11. A comparison between the light output power of micro-cylinder-structured LEDs of different height and conventional LEDs

4.2 The photonic crystal effect

The behavior of an electromagnetic wave traveling in a homogeneous medium can be obtained by solving the Helmholtz equation (the Helmholtz equation is derived from Maxwell's equations). The Helmholtz equation is:

$$\nabla^2 E + k^2 E = 0$$

where E is the electromagnetic wave and k is the wave number. Combined with the boundary conditions, Helmholtz equation can be solved via a harmonic solution. While solving for the equation, the wave number, frequency ($\omega = 2\pi \times \nu$), permittivity (ϵ), and permeability (μ) must satisfy below equation:

$$k^2 = \omega^2 \mu \epsilon$$

In an ideal non-dispersive medium, the permittivity and permeability are independent of the frequency of the electromagnetic wave. Therefore, a linear relation between the wave number and the frequency exists. However, nearly all media are dispersive to a certain extent. That is, the permittivity and permeability are dependent on the frequency and lead to a nonlinear relation between the wave number and the frequency. In such a case, the group velocity and the phase velocity of the wave would not be the same.

When the medium (where the electromagnetic wave travels in) is a periodic structure in space with a periodicity comparable to the wavelength of the wave, the permittivity can also be regarded as a periodic distribution (Bloch's theorem) in space (assuming the permeability is 1). Though solving the Helmholtz equation in these periodic medium results in a harmonic solution that is similar to above equation, this solution carries the information of the periodic structure of the medium. The photonic crystal is a medium with such a periodically distributed permittivity, and the spatial periodicity of a photonic crystal is slightly smaller than the wavelength of the wave.

The solution to Helmholtz equation can be affected by the following factors: polarization of the electromagnetic wave, the interaction length between the electromagnetic wave and the photonic crystal, and the permittivity difference between the periodic structure and the substrate. Therefore, when the electromagnetic wave enters the photonic crystal, different eigen modes are formed, capable of interfering constructively or destructively to create energy bands. If the eigen modes form destructive interference in a specific direction, such a phenomenon is called the photonic band gap.

Because the existence of the photonic band gap is related to the frequency and the propagation direction of the electromagnetic wave, the photonic band gap can be used as a reflector for the large angle bending of electromagnetic wave propagation in integrated optics. Applying the photonic crystal to the LED chip can manipulate the directions of emitted photons. When the photonic crystal structure suppresses the photons with large emitting angular, the LED can be approximated a collimated light source. Conversely, when the photonic crystal structure suppresses the photons with small angular, the LED behaves akin to an expansion light source. This is the underlying principle of the far-field light pattern effect found in the photonic crystal. In addition to the far-field effect, the photonic crystal can be used to form a photonic bandgap within the active region of the LED. In this manner, photons generated by the active region are forced to escape the active region promptly, hence increasing the light-extraction efficiency [31]. If the photonic crystal is applied to the LED surface, high order diffraction lights are generated by the momentum compensation that occurred during the interaction of the photonic crystal and the guided photons. The otherwise confined photons in the LED can be coupled to the free space by the diffraction, which is another means to improve the light-extraction efficiency of the LED. Researchers at U.C. Santa Barbara conducted a series of discussions regarding the photonic crystal effect [32-35].

Analyzing the escape paths of the emitted photons from LEDs provided the observation that the chip surface's escape photons comprise 12 % of photons generated in the active region when a highly reflective coating is applied to the sapphire substrate. Approximately 22 % of the photons are confined within the sapphire substrate, while 66 % of the trapped photons are located in the chip region. Trapped photons, confined in the air/sapphire/GaN interfaces, are known as guided light. A longer interaction length between the photonic crystals and emitted photons typically results in an increased optical modulation effect on the guided light.

The significant difference (1.4) between GaN and air refraction indices makes the GaN/air interface an excellent waveguide material, which confines photons of the active region within the GaN. Photonic crystals are used to extract the guided light into the air. Considering diffraction, the guided light-extraction efficiency is dependent on the mode of the confined photons. Photons of lower order modes are confined to the center of GaN, and prevented from interacting with the photonic crystal structures on the chip's surface, which leads to inefficient photon diffraction of the lower-order modes and limits improvements to light-extraction efficiency.

A shallow photonic crystal layer on the GaN surface slightly affects the diffraction efficiency of the guided light, and therefore, the photonic crystal structure is typically 1 μm in thickness to enhance the interaction between the photonic crystal and the guided photons. However, a deep photonic crystal layer has a reduced effective refractive index, resulting in rapid evanescence of the lower-order modes in the photonic crystal. In such circumstances, the light-extraction efficiency cannot be improved. To improve the efficiency of the shallow photonic crystal layer, David et al. [32] inserted a low-refractive index material $\text{Al}_x\text{Ga}_{1-x}\text{N}$ in the GaN to couple the lower-order photons trapped in the center of the GaN buffer layer to the GaN cap layer (Figure 12.). The diffraction efficiency of the lower-order photons substantially improved upon inserting the $\text{Al}_x\text{Ga}_{1-x}\text{N}$.

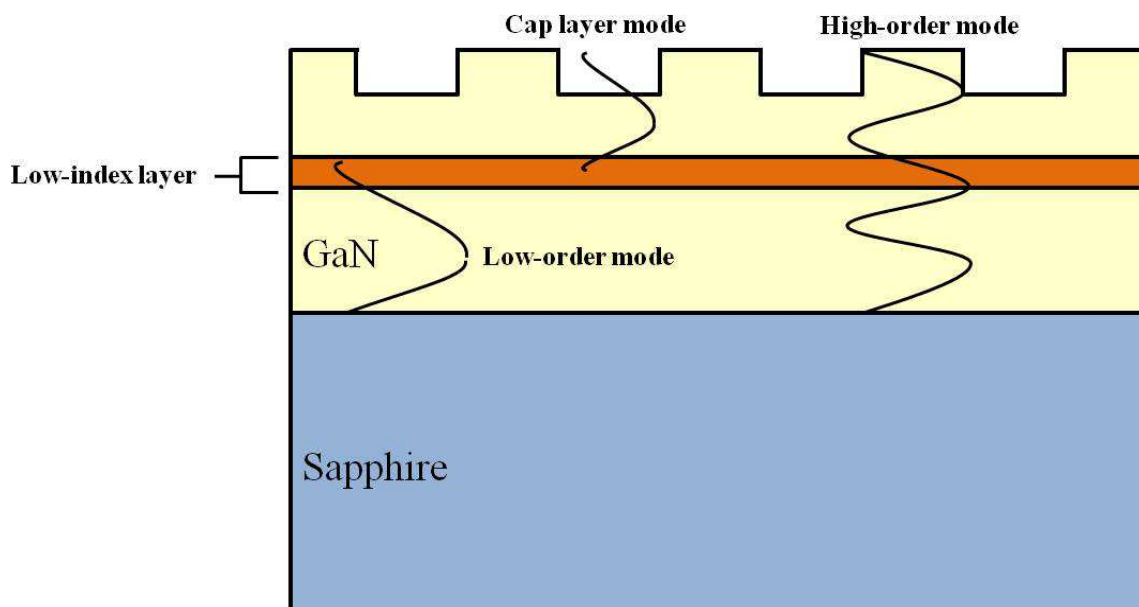


Fig. 12. Insert a low-index layer to improve mode coupling with photonics crystal

An LED is a light-emitting device comprising point light sources that emit photons in random directions. Therefore, an omnidirectional light-extraction structure reflects photons with various modes and directions from the active layer to outside the GaN, would be an ideal photonic crystal structure. To achieve the isotropic light extraction, the photonic band gap in the various directions must be of equal efficiency. Numerous photonic crystal structures designed to achieve the aforementioned objective have been proposed, including Archimedean tilings [36], Penrose lattices [37-39] and quasicrystals [40-43]. Expanding on previous discussions regarding photonic crystals, David et al. [33] used A7 Archimedean tilings as the photonic crystal layer on GaN LEDs. The A7 photonic crystal was composed of

a triangular lattice and a complex basis. The unit cell is formed by 7 holes, and a is the hole interval. The lattice constant of photonic crystals $b = a(1 + \sqrt{3})$. Applying this photonic crystal structure to the surface of GaN LEDs resulted in a high order crystal, thereby diffracting the light into air, instead of onto the substrate. Diffraction occurred in the various Brillouin zone of the reciprocal lattice, demonstrating the omnidirectionality of the A7 structure.

Shields et al. [44] used the higher rotational symmetry of the photonic quasicrystals (PQCs) to achieve omnidirectionality. The designed PQCs patterns were based on square-triangular tiling using three different pitches: 450, 550, and 750 nm. Shield's experiments revealed a plateau on the far-field profile that was independent of the measurement angle. The finite-difference time-domain (FDTD) simulation also demonstrated similar behavior.

Increasing light-extraction efficiency and adjusting the emission profile can be achieved simultaneously by optimizing the coupling distance between the emitted photon and the photonic crystal. The momentum of photons parallel to the photonic crystal plate are coupled with the reciprocal lattice constant of the photonic crystal via the diffraction effect, generating photons with momentum perpendicular to the photonic crystal plate. Using an appropriate reciprocal lattice constant can increase the number of photons within the escape cone. An LED emission profile can also be adjusted using the same approach [34]. A triangular lattice photonic crystal is applied to both transparent electrodes of the LED. On the ITO side, the depth and the area of the photonic crystal is 120 nm and $400 \times 400 \mu\text{m}^2$, respectively. On the Ni/Au side, the depth and the area of the photonic crystal is 250 nm and $500 \times 500 \mu\text{m}^2$, respectively. The lattice constants of the photonic crystal are 185, 200, 215, and 230 nm. The experiment demonstrated that the vertical emission profile peaks occur at the second order diffraction (periodicity of photonic crystals/wavelength=0.5), and corresponds to 215 nm of lattice period/430 nm in ITO thickness, and 200 nm of lattice period/405 nm in Ni/Au thickness. Changing the lattice constant altered the vertical emission of various modes. In this sample, the extraction of cap layer mode photons into air was evident.

Methods to modulate the far-field light patterns and to improve the light-extraction efficiency of LEDs using sub-microstructures lead to that most photons confined within the LED can be coupled outside the LED, using photonic crystals. Therefore, coupling photons to the escaping cone is a major mechanism enabling photonic crystals to improve the light extraction efficiency and to adjust the far-field light pattern. Though the depth, the lattice constant and the filling factors of the photonic crystal adjust the mode of the trapped photons to enter the air lightline, the polarization and propagation directions of the photons interacting with the photonic crystals require consideration. Photons generated by the spontaneous emission process in the LED have poor temporal and spatial coherences, and therefore, the roughening effect caused by the photonic crystal should also be considered.

Numerous studies have investigated the application of nanoimprinted photonic crystals in LEDs. Examples are listed below:

Cho et al. [45] used the nanoimprint lithography and ICP etching to fabricate photonic crystal structures of various depths onto the ITO/GaN surface of a $375 \mu\text{m} \times 330 \mu\text{m}$ blue LED chip. Upon optical efficiency optimization, the efficiency of the packaged LED can be further enhanced by 25 %, using a 20 mA current injection. Using the 3D-FDTD simulation, light-extraction efficiency increases in correlation with the etching depth of the photonic crystals. However, the light-extraction efficiency decreases when the ratio (wavelength/effective refractive index) is exceeded.

Cheng et al. [46] applied the photonic crystal [$1 \times 1 \text{ mm}^2$] to the green power chip and combined the omnidirectional reflector at the back of the chip. The overall efficiency increased by 88 %, with a collimated far-field light pattern.

Nao et al. [47] attached a photonic crystal in a triangular lattice (diameter=100~250 nm, height=120 nm) to the flip chip between the sapphire and the GaN, allowing the diffractive coupling of photons to enter the air from the back of the sapphire substrate. The far-field pattern was collimated, and a lobe was observed near the horizontal direction. The lobe was attributed to the intermixing of light emitted from the side and front of the chip.

Huang et al. [48] applied quasi-photonic crystals to both n- and p-GaN layers in a vertical LED. The optical efficiency exceeded that of a single photonic crystal LED.

Byeon et al. [49] created a hexagonal array of holes with a diameter of 250 to 380 nm and 600 to 900 nm of pitch as the photonic crystal layer on the ITO of a green LED, using soft imprint technology (to prevent damages on the GaN LED). The light emitting efficiency improved maximally by 25 % under a 20 mA current injection.

Khokhar et al. [50] compared e-beam lithography and nanoimprinting technology concerning the creation of photonic crystal structures. Though the e-beam lithography created a more precise and accurate pattern, it is not suitable for mass production, and while nanoimprinting technology is suitable for mass production, several issues remain. For example, the residual layer must be removed using etching, which limits the practical thickness of the photonic crystal layer, and the imprint material requires a high-etching selectivity.

The photonic crystal structure can be applied quickly and accurately to the surface and the interior of the LED via the nanoimprint lithography technique [51, 52]. However, because the electrical characteristics of the LED will be degraded using dry etching of the p-GaN, T. A. Truong et al. [53] applied sol gel titania to the substrate (soft imprint plus a 300 °C solidification process) to form titanium oxide photonic crystal structures on the LED without damaging the LED surface.

Motivated by the great potential of photonic crystal application on LED, several equipment manufacturers have devised intriguing strategies to develop this field. Molecular imprints Inc. [54] sprays the imprint material to a 6" quartz substrate. Using a step-and-repeat exposure procedure, they progressively transfer the structure of a hard mother mold ($5 \times 5 \text{ mm}^2$) to the entire area of the quartz substrate, which now acts as a substitute mold. The nanoimprint of the 3" GaN LED occurs from the quartz mold. Due to the hard imprint nature of this technique, the cleanness of the mold and the substrate play crucial roles. Suss MicroTec Lithography GmbH [55] uses a PDMS soft mold adhered to the substrate by the vacuum force before imprinting. To prevent trapping air between the mold and the substrate during imprinting, the PDMS mold is gradually released from the vacuum force until the mold and the imprinting material are held together by the capillary force. After UV exposure, the gradual vacuum force removes the mold once more. EV Group Inc. [56] also adopted PDMS molds. The difference is that the mold comprises two soft PDMS layers with different degrees of hardness. The harder layer is the outer layer that directly touches the imprinting materials, which is believed to solve the rigidity issue of a typical soft mold, and prevent the deformation of the mold. Obducat AB [57] uses non-reusable polymer stamp as the mold. The polymer stamp is fabricated by pressing a hard master stamp against the polymer film. Once the polymer stamp is used, it is disposed. Due to its single usage nature, the stamp has no lifetime issues. In addition, the flexibility of the polymer stamp allows

them to be applied to nonplanar surfaces. Obducat's solution has already found a significant number of industrial users, including two LED manufacturers from Taiwan, Luxtalek and Epistar.

4.3 The Effects of NPSS

NPSS has three distinct advantages:

1. Enhancing the light extraction efficiency

The PSS on the micrometer scale has been experimentally demonstrated to improve the light extraction efficiency of LEDs significantly. Further shrinking the size of PSS can increase the structural density, and hence, enhancing the light extraction efficiency even more.

2. Simplifying the process parameters

Changing the condition on the current micron scale PSS process usually requires careful/ tedious optimization of the subsequent epitaxial process parameters. By shrinking the patterning size into nanoscales, this optimization step can be neglected, facilitating a more rapid LED growth process.

3. Reducing the thickness of the buffer layer

A thick buffer layer is typically necessary to smooth out the PSS patterned surface prior to the epitaxy process. If the size of the PSS structures is in nanoscales, the required buffer layer is thin and may be achieved by the side growth of the epitaxial layer, streamlining the LED growth process and increasing the process yield.

Huang et al. [58] created polymer nanostructures on the sapphire substrate using the thermal pressing technique. The imprint material also acted as the resist layer for the ICP etching process. A concave NPSS pattern was obtained with a periodicity of 450 nm, a diameter of 240 nm, and a depth of 165 nm. SEM measurements showed that the GaN did not fulfill the the NPSS holes completely, causing a hole array at the GaN/NPSS interface. Due to the difference in the refraction indices between these holes and the surrounding matrix, the light originating from the MQW underwent scattering and multiple reflections at the GaN/NPSS interface. The light was bounced back to the GaN/Air interface, increasing the likelihood of light escaping the LED. Under a 20 mA electrical current injection, the NPSS was found to enhance the light extraction efficiency by as much as 1.33 times that of conventional LEDs. Huang et. al. [59] used a similar thermal pressing technique combined with ICP etching to create a convex NPSS with a periodicity of 750 nm and a diameter of 450 nm. The height of the NPSS structures was 182 nm. Under a 20 mA electrical excitation, the 300×300 μm² NPSS had 35% more light-extraction efficiency compared to conventional LEDs. If the quasi-photonic crystal effect were considered, the efficiency could be further increased to 48%. C.C. Kao et al. [60] used a similar process for creating NPSS to study the dependence of the light extraction on the aspect ratios of the NPSS. Their experiment showed that efficiency was higher for higher aspect ratios. The efficiency was increased from 11% to 27% for aspect ratios from 2.00 to 2.50, respectively.

Results from the micron scale PSS structures shows that increasing the aspect ratio of the PSS can also increase the light-extraction efficiency. However, the height of the ICP-etched NPSS is directly related to the size of the nanoimprinted polymer structures. Due to the high mechanical strength and the sound chemical stability, the etching selective ratio between the sapphire and the polymer resist is small, resulting in a less than desired etching depth on the sapphire substrate. Figure 13 shows the NPSS structures etched by the sulfuric acid and the phosphoric acid at high temperatures. The periodicity is 1.25 μm and the depth is 340 nm.

nm. A thin layer of silicon oxide is used as the etching resist at high temperatures. If the etching time is long, the PSS pattern transforms into cylindrical rods with a maximum height of 700 nm (Figure 14). With the ICP etching process using an Ni thin film as the resist layer, an even higher cylindrical rod can be obtained due to the higher etching selective ratio between the sapphire and the Ni, as shown in Figure 15. [61].

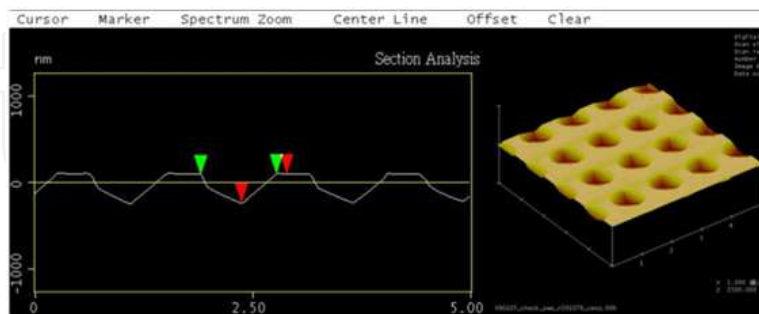


Fig. 13. AFM images of concave NPSS formed using wet etching

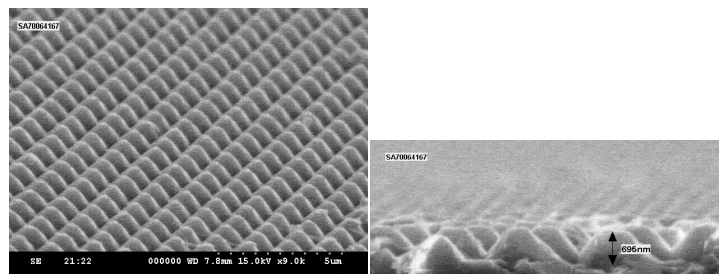


Fig. 14. SEM images of convex NPSS formed using wet etching

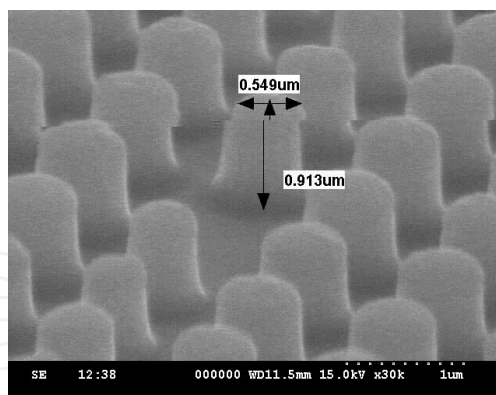


Fig. 15. SEM images of dry etched cylinder NPSS

Hsieh et al. [62] created NPSS via a thermal nanoimprint technique, using Ni as the resist layer. A anti-adhesive layer (1H, 1H, 2H, and 2H-perfluorooctyltrichlorosilane) was coated on the mold, followed by a thin Ni layer. A layer of PMMA was sprayed onto the substrate. The Ni layer on the protrudent mold was peel-off before being transferred to the PMMA, using thermal pressing. NPSS ($\sim 0.4 \mu\text{m}$ depth) was then created via ICP etching. The diameters were 0.4, 0.6, 0.8, 1.0, 2.0, and $3.0 \mu\text{m}$, with the corresponding EL intensity of 128.4, 120.2, 109.2, 102.5, 91.6, 90.3, and 69.5 mcd, respectively. In comparison to the unpatterned substrate, the efficiency of the NPSS ($0.4 \mu\text{m}$) LED was increased by 84.7%.

5. Conclusion

Nanotechnology is typically defined as the fabrication of structures under 100 nm. The fabrication of structures between 100 nm~999 nm is referred to as sub-micron technology. However, much literature related to LEDs referring to the sub-micron process as nanotechnology exists. Therefore, this study referred to the nanoimprint as the fabrication of several hundred nanometer structures via the imprint technique, nonetheless indicating that the few hundred-nanometer fabrication process is applicable to the industry. This scale is suitable for the development of the nanoimprint technique because the limitation of optical lithography does not affect it, and the technique is low cost compared to the expensive advanced projection lithography and the electron beam lithography. The LED chip has a 0~10 μm bow and the epitaxy is usually processed under a temperature near 1000°C. Because the coefficients of thermal expansion of the substrate and the GaN epitaxial layer are different, the epitaxy process is likely to cause the deformation of the chip. Moreover, due to (a) the cleanness issues, (b) surface defects of the epitaxial layer, and (c) the emphasis on the height of the electrode after the chip process, the imprint process of the entire wafer is rendered difficult. Therefore, the use of a flexible soft mold is crucial.

This article presents the nanoimprinting technique integrated with the conventional LED fabrication process. Due to its low cost, simplicity, easy integration, and the enhancement of the optical efficiency, nanoimprinting has a widespread application in various industries. The future business aspect of nanoimprint technology is dependent on the development of manufacturing equipment suitable for LEDs fabrication.

6. References

- [1] M. R. Krames, G. E. Höfler, E. I. Chen, I. H. Tan, P. Grillot, N. F. Gardner, H. C. Chui, J. W. Huang, S. A. Stockman, F. A. Kish, and M. G. Craford, "High power truncated inverted pyramid $\text{Al}_x\text{Ga}_{12x}\text{In}_{0.5}\text{P}/\text{GaP}$ light-emitting diodes exhibiting >50% external quantum efficiency", *Applied physics letters*, Vol. 75, pp. 2365, 1999.
- [2] C. F. Lin, Z. J. Yang, B. H. Chin, J. H. Zheng, J. J. Dai, B. C. Shieh, and C. C. Chang, "Enhanced light output power in InGaN light-emitting diodes by fabricating inclined undercut structure", *Journal of The Electrochemical Society*, Vol. 153, pp. 1020, 2006.
- [3] C. E. Lee, Y. C. Lee, H. C. Kuo, M. R. Tsai, T. C. Lu, and S. C. Wang, "High brightness GaN-based flip-chip light-emitting diodes by adopting geometric sapphire shaping structure", *Semiconductor science and technology*, Vol. 23, pp. 025015, 2008.
- [4] C. Huh, K. S. Lee, E. J. Kang, and S. J. Park, "Improved light-output and electrical performance of InGaN-based light-emitting diode by microroughening of the p-GaN surface", *Journal of Applied Physics*, Vol. 93, pp.9383, 2003.
- [5] T. Fujii, Y. Gao, R. Sharma, E. L. Hu, S. P. DenBaars, and S. Nakamura, "Increase in the extraction efficiency of GaN-based light-emitting diodes via surface roughening," *Applied physics letters*, Vol.84, pp. 6, 2004.
- [6] T. X. Lee, K. F. Gao, W. T. Chien, and C. C. Sun, "Light extraction analysis of GaN-based light-emitting diodes with surface texture and/or patterned substrate", *Optics Express* Vol. 15 pp. 6670, 2007.

- [7] T. X. Lee, K.F. Go, T. Y. Chung, and C. C. Sun, "Light extraction analysis of GaN-based LEDs", *Proceeding of SPIE* Vol. 6473, pp. 64731P-1, 2007.
- [8] K. Tadatomo, and T. Taguchi, "High output power InGaN ultraviolet light emitting diodes fabricated on patterned substrates using metal organic vapor phase epitaxy," *Japanese Journal of Applied Physics*, Vol. 40, pp. L583, 2001.
- [9] M. Yamada, T. Mitani, Y. Narukawa, S. Shioji, I. Niki, S. Sonobe, K. Deguchi, M. Sano, and T. Mukai, "InGaN-based near-ultraviolet and blue-light-emitting diodes with high external quantum efficiency using a patterned sapphire substrate and a mesh electrode," *Japanese Journal of Applied Physics*, Vol. 41, pp. L1431, 2002.
- [10] A. Bell, R. Liu, F. A. Ponce, H. Amano, I. Akasaki, and D. Cherns, "Light emission, and microstructure of Mg-doped AlGaIn grown on patterned sapphire," *Applied Physics Letters*, Vol. 82, pp. 349, 2003.
- [11] K. T. Lee, Y. C. Lee, and J. Y. Chang, "Characterization of Gallium Nitride Grown on Patterned Sapphire Substrate with Shallow U-Shaped Stripe Grooves", *Journal of The Electrochemical Society*, Vol. 155, pp. H673, 2008,
- [12] E. Yablonovitch, "Inhibited Spontaneous Emission in Solid-State Physics and Electronics", *Physical Review Letters*, Vol. 58, pp. 2059, 1987.
- [13] S. John, "Strong localization of photons in certain disordered dielectric superlattices", *Physical Review Letters*, Vol. 58, p.2486-2489, 1987.
- [14] M. Akanegawa, Y. Tanaka, and M. Nakagawa, "Basic study on traffic information system using LED traffic lights," *IEEE Transactions on Intelligent Transportation Systems*, Vol. 2, pp. 197, 2001.
- [15] H. Ghafoori-Shiraz, "Butt coupling efficiency of long-wavelength edge-emitting LEDs to single-mode fibers", *Transactions of the Institute of Electronics, Information and Communication Engineers, Section E*, Vol. E70, pp. 617, 1987.
- [16] Y. Tu, S. Jin, Y. Wang, and L. Dou, "Color uniformity and data simulation in high-power RGB LED modules using different LED-chips arrays," *Proceeding of SPIE*, Vol. 6828, pp. 682816, 2007.
- [17] S. Y. Chou, P. R. Krauss and P. J. Renstrom, "Imprint of sub-25 nm vias and trenches in polymers", *Applied Physics letters*, Vol. 67, pp. 3114, 1995.
- [18] M. Bender, M. Otto, B. Hadam, B. Vratzov, B. Spangenberg and H. Kurz, "Fabrication of nanostructures using a UV-based imprint technique", *Microelectronic Engineering*, Vol. 53, pp. 233, 2000.
- [19] Y. Xia and G. M. Whitesides, "Soft Lithography", *Annual Review of Materials Science*, Vol. 28, pp. 153, 1998.
- [20] C. Peng and S. W. Pang, "Hybrid mold reversal imprint for three-dimensional and selective patterning", *Journal of Vacuum Science and Technology B: Microelectronics and Nanometer Structures*, Vol. 24, pp. 2968, 2006.
- [21] H. Tan, A. Gilbertson, and S. Y. Chou, "Roller nanoimprint lithography," *Journal of Vacuum Science and Technology B: Microelectronics and Nanometer Structures*, Vol. 16, pp. 3926, 1998
- [22] M. T. Gale, "Replication technique for diffractive optical elements", *Microelectronic Engineering*, Vol. 34, pp. 339, 1997.

- [23] T. Makela, T. Haatainen, P. Majander, J. Ahopelto, and V. Ambertini, "Continuous double-sided roll-to-roll imprinting of polymer film," *Japanese Journal of Applied Physics*, Vol. 47, pp. 5142, 2008.
- [24] Y. C. Lee, B. T. Chen, and T. H. Wu, "Fabrication of SU-8 microstructures by roller imprinting technique to enhance light extraction efficiency of LEDs", *Proceedings of the 6th International Conference on MicroManufacturing*, pp. 73, Tokyo, Mar. 7-10, 2011.
- [25] C. H. Chen, Y. C. Lee, C. D. Chen, S. J. Lai, and S. J. Liaw, "Roller imprinting based on focus infrared heating," *Proceedings of the 3rd IEEE Int. Conf. on Nano/Micro Engineered and Molecular Systems*, Sanya, China, 2008.
- [26] S. J. Chang, C. F. Shen, W. S. Chen, C. T. Kuo and T. K. Ko, S. C. Shei, and J. K. Sheu, "Nitride-based light emitting diodes with indium tin oxide electrode patterned by imprint lithography," *Applied Physics Letters*, Vol. 91, pp. 013504, 2007.
- [27] H. W. Huang, C. H. Lin, C. C. Yu, B. D. Lee, C. H. Chiu, C. F. Lai, H. C. Kuo, K. M. Leung, T. C. Lu, and S. C. Wang, "Enhanced light output from a nitride-based power chip of green light-emitting diodes with nano-rough surface using nanoimprint," *Nanotechnology*, Vol. 19, pp. 185301, 2008.
- [28] W. Zhou, G. Min, Z. Song, J. Zhang, Y. Liu and J. Zhang, "Enhanced efficiency of light emitting diodes with a nano-patterned gallium nitride surface realized by soft UV nanoimprint lithography", *Nanotechnology*, Vol. 21, pp. 1, 2010.
- [29] Y. C. Lee, M. J. Ciou, and J. S. Huang, "Light output enhancement for nitride-based light emitting diodes via imprinting lithography using spin-on glass", *Microelectronics Engineering*, Vol. 87, No. 11, pp. 2211, 2010.
- [30] Y. C. Lee, M. J. Ciou, and J. S. Huang, "The influence of nanoimprinting surface structures on the optical efficiency of GaN-based LEDs", *IEEE Transactions on Nanotechnology*, in press, 2010.
- [31] S. Fan, P. R. Villeneuve and J. D. Joannopoulos, "High extraction efficiency of spontaneous emission from slabs of photonic crystals", *Physical review letters*, Vol. 78, pp.3294, 1997.
- [32] A. David, T. Fujii, E. Matioli, R. Sharma, S. Nakamura, S. P. DenBaars, and C. Weisbuch, "GaN light-emitting diodes with Archimedean lattice photonic crystals," *Applied Physics Letters* Vol. 88, pp. 073510, 2006.
- [33] A. David, T. Fujii, E. Matioli, R. Sharma, S. Nakamura, S. P. DenBaars, and C. Weisbuch, "Photonic-crystal GaN light-emitting diodes with tailored guided modes distribution," *Applied Physics letters*, Vol. 88, pp.061124, 2006
- [34] K. McGroddy, A. David, E. Matioli, M. Iza, S. Nakamura, S. DenBaars, J. S. Speck, C. Weisbuch, and E. L. Hu, "Directional emission control and increased light extraction in GaN photonic crystal light emitting diodes", *Applied Physics Letters*, Vol. 93, pp. 103502, 2008.
- [35] T. A. Truong, L. M. Campos, E. Matioli, I. Meinel, C. J. Hawker, C. Weisbuch, and P. M. Petroff, "Light extraction from GaN-based light emitting diode structures with a noninvasive two-dimensional photonic crystal", *Applied Physics Letters*, Vol. 94, pp. 023101, 2009.

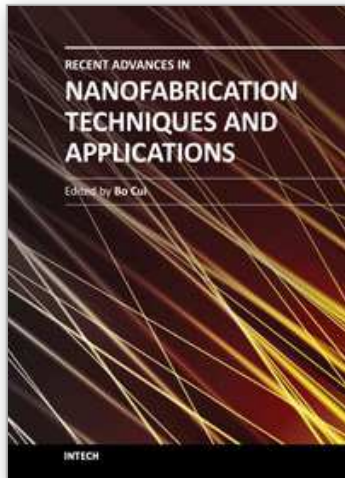
- [36] S. David, A. Chelnokov, and J.-M. Lourtioz, "Isotropic photonic structures: archimedean-like tilings and quasi-crystals", *IEEE Journal of Quantum Electronics*, Vol. 37, pp. 1427, 2001.
- [37] A. D. Villa, S. Enoch, G. Tayeb, V. Pierro, V. Galdi, and F. Capolino, "Band gap formation and multiple scattering in photonic quasicrystals with a penrose-type lattice", *Physical Review Letters*, Vol. 94, pp. 183903, 2007.
- [38] S. P. Gorkhali, J. Qi, and G. P. Crawford, "Electrically switchable meso scale penrose quasi crystal structure", *Applied Physics Letters*, Vol. 86, pp. 011110, 2005.
- [39] M. Notomi, H. Suzuki, T. Tamamura, and K. Edagawa, "Lasing action due to the two-dimensional quasiperiodicity of photonic quasicrystals with a penrose lattice", *Physical Review Letters*, Vol. 92, pp. 123906, 2004.
- [40] Y. S. Chan, C. T. Chan, and Z. Y. Liu, "Photonic band gaps in two dimensional photonic quasicrystals", *Physical Review Letters*, Vol. 80, pp. 956, 1998.
- [41] M. E. Zoorob, M. D. B. Charlton, G. J. Parker, J. J. Baumberg, and M. C. Netti, "Complete photonic band gaps in 12-fold symmetric quasi crystals", *Nature*, Vol. 404, pp. 740, 2000.
- [42] P. L. Hagelstein and D. R. Denison, "Nearly isotropic photonic bandgap structures in two dimensions", *Optics Letters*, Vol. 24, pp. 708, 1999.
- [43] J. Zarbakhsh, F. Haggmann, S. F. Mingaleev, K. Busch, and K. Hinger, "Arbitrary angle waveguiding applications of two-dimensional curvilinear-lattice photonic crystals", *Applied Physics Letters*, Vol. 84, pp. 4687, 2004.
- [44] P. A. Shields, M. D. B. Charlton, T. Lee, M. E. Zoorob, D. W. E. Allsopp, and W. N. Wang, "Enhanced light extraction by photonic quasi-crystals in GaN blue LEDs", *IEEE Journal of Selected Topics in Quantum Electronic*, Vol. 15, pp. 1269, 2009.
- [45] H. K. Cho, J. Jang, J. H. Choi, J. Choi, J. Kim, J. S. Lee, B. Lee, Y. Ho Choe, K. D. Lee, S. H. Kim, K. Lee, S. K. Kim, and Y. H. Lee, "Light extraction enhancement from nanoimprinted photonic crystal GaN-based blue light emitting diodes", Vol. 14, *Optics Express*, pp. 8654, 2006.
- [46] B. S. Cheng, C. H. Chiu, K. J. Huang, C. F. Lai, H. C. Kuo, C. H. Lin, T. C. Lu, S. C. Wang and C. C. Yu, "Enhanced light extraction of InGaN-based green LEDs by nano-imprinted 2D photonic crystal pattern", *Semiconductor Science Technology*, Vol. 23, pp. 055002, 2008.
- [47] Y. Naoi, M. Matsumoto, T. Tan, M. Tohno, S. Sakai, A. Fukano, and S. Tanaka, "GaN-based light emitting diodes with periodic nano-structures on the surface fabricated by nanoimprint lithography technique", *Physica Status Solidi C*, Vol. 7, pp. 2154, 2010.
- [48] H. W. Huang, C. H. Lin, Z. K. Huang, K. Y. Lee, C. C. Yu, and H. C. Kuo, "Double photonic quasi-crystal structure effect on GaN-based vertical-injection light-emitting diodes", *Japanese Journal of Applied Physics* Vol. 49 pp. 022101, 2010.
- [49] K. J. Byeon, H. Park, J. Y. Cho, K. Y. Yang, J. H. Baek, G. Y. Jung, and H. Lee, "Fabrication of photonic crystal structure on indium tin oxide electrode of GaN-based light-emitting diodes", *Physica Status Solidi A*, Vol. 208, pp. 480, 2011.

- [50] A. Z. Khokhar, K. Parsons, G. Hubbard, F. Rahman, D. S. Macintyre, C. Xiong, D. Massoubre, Z. Gong, N. P. Johnson, R. M. De La Rue, I. M. Watson, E. Gu, M. D. Dawson, S. J. Abbott, M. D. B. Charlton, M. Tillin, "Nanofabrication of gallium nitride photonic crystal light-emitting diodes", *Microelectronic Engineering* Vol. 87, pp. 2200, 2010.
- [51] K. D. Lee, S. H. Kim, J. D. Park, J. Y. Kim and S. J. Park, "Application of nanoimprint lithography to nano-optics: wire grid polarizer and photonic crystal LED", *Proceedings of SPIE*, Vol. 6462, pp. 64620P-1, 2007.
- [52] B. S. Cheng, C. H. Chiu, K. J. Huang, C. F. Lai, H. C. Kuo, C. H. Lin, T. C. Lu, S. C. Wang, and C. C. Yu, "Enhanced light extraction of InGaN-based green LEDs by nano-imprinted 2D photonic crystal pattern", *Semiconductor Science and Technology*, Vol. 23, pp. 055002, 2008.
- [53] T. A. Truong, L. M. Campos, E. Matioli, I. Meinel, C. J. Hawker, C. Weisbuch, and P. M. Petroff, "Light extraction from GaN-based light emitting diode structures with a noninvasive two-dimensional photonic crystal", *Applied Physics Letters* Vol. 94, pp. 023101, 2009.
- [54] R. Hershey, G. Doyle, C. Jones, D. LaBrake, and Mike Miller, "Imprint lithography advances in LED manufacturing", *Physica Status Solidi C*, Vol. 4, pp. 21, 2007.
- [55] R. Ji, M. Hornung, M. A. Verschuuren, R. van de Laar, J. van Eekelen, U. Plachetka, M. Moeller, and C. Moormann, "UV enhanced substrate conformal imprint lithography (UV-SCIL) technique for photonic crystals patterning in LED manufacturing", *Microelectronic Engineering* Vol. 87, pp. 963, 2010.
- [56] M. Bender, U. Plachetka, J. Ran, A. Fuchs, B. Vratzov, H. Kurz, T. Glinsner, and F. Lindner, "High resolution lithography with PDMS molds", *Journal of Vacuum Science and Technology B: Microelectronics and Nanometer Structures*, Vol. 22, pp. 3229, 2004.
- [57] "NanoImprint Lithography: Ready for high volume manufacturing", *Euro Asia Semiconductor*, v 29, pp. 15, 2007.
- [58] H. W. Huang, C.H. Lin, J.K. Huang, K.Y. Lee, C.F. Lin, C.C. Yu, J.Y. Tsai, R. Hsueh, H.C. Kuo, S. C. Wang, "Investigation of GaN-based light emitting diodes with nano-hole patterned sapphire substrate (NHPSS) by nano-imprint lithography", *Materials Science and Engineering B* Vol. 164, pp. 76, 2009.
- [59] H. W. Huang, J. K. Huang, S. Y. Kuo, K. Y. Lee, and H. C. Kuo, "High extraction efficiency GaN-based light-emitting diodes on embedded SiO₂ nanorod array and nanoscale patterned sapphire substrate", *Applied Physics Letters*, Vol. 96, pp. 263115, 2010.
- [60] C. C. Kao, Y. K. Su, C. L. Lin, and J. J. Chen, "The aspect ratio effects on the performances of GaN-based light-emitting diodes with nano patterned sapphire substrates", *Applied Physics Letters*, Vol. 97, pp. 023111, 2010.

- [61] H. J. Horng, "A Study of Submicron Patterned Sapphire Substrates Applied to GaN-based Light-Emitting Diode", Master thesis, Chung Yuan Christian University, Taiwan, 2010.
- [62] E. D. Hsieh and Y. C. Lee, "Contact transfer and metal mask embedded lithography apply to fabricate patterned sapphire substrate", The 14th Nano and Micro-System Technology Conference, Kaohsiung, Taiwan, 2010.

IntechOpen

IntechOpen



Recent Advances in Nanofabrication Techniques and Applications

Edited by Prof. Bo Cui

ISBN 978-953-307-602-7

Hard cover, 614 pages

Publisher InTech

Published online 02, December, 2011

Published in print edition December, 2011

Nanotechnology has experienced a rapid growth in the past decade, largely owing to the rapid advances in nanofabrication techniques employed to fabricate nano-devices. Nanofabrication can be divided into two categories: "bottom up" approach using chemical synthesis or self assembly, and "top down" approach using nanolithography, thin film deposition and etching techniques. Both topics are covered, though with a focus on the second category. This book contains twenty nine chapters and aims to provide the fundamentals and recent advances of nanofabrication techniques, as well as its device applications. Most chapters focus on in-depth studies of a particular research field, and are thus targeted for researchers, though some chapters focus on the basics of lithographic techniques accessible for upper year undergraduate students. Divided into five parts, this book covers electron beam, focused ion beam, nanoimprint, deep and extreme UV, X-ray, scanning probe, interference, two-photon, and nanosphere lithography.

How to reference

In order to correctly reference this scholarly work, feel free to copy and paste the following:

Yeeu-Chang Lee and Sheng-Han Tu (2011). Improving the Light-Emitting Efficiency of GaN LEDs Using Nanoimprint Lithography, Recent Advances in Nanofabrication Techniques and Applications, Prof. Bo Cui (Ed.), ISBN: 978-953-307-602-7, InTech, Available from: <http://www.intechopen.com/books/recent-advances-in-nanofabrication-techniques-and-applications/improving-the-light-emitting-efficiency-of-gan-leds-using-nanoimprint-lithography>

INTECH
open science | open minds

InTech Europe

University Campus STeP Ri
Slavka Krautzeka 83/A
51000 Rijeka, Croatia
Phone: +385 (51) 770 447
Fax: +385 (51) 686 166
www.intechopen.com

InTech China

Unit 405, Office Block, Hotel Equatorial Shanghai
No.65, Yan An Road (West), Shanghai, 200040, China
中国上海市延安西路65号上海国际贵都大饭店办公楼405单元
Phone: +86-21-62489820
Fax: +86-21-62489821

© 2011 The Author(s). Licensee IntechOpen. This is an open access article distributed under the terms of the [Creative Commons Attribution 3.0 License](#), which permits unrestricted use, distribution, and reproduction in any medium, provided the original work is properly cited.

IntechOpen

IntechOpen